Acta Crystallographica Section D
Biological Crystallography
ISSN 0907-4449

A benzoic acid inhibitor induces a novel conformational change in the active site of *Influenza B virus* neuraminidase

Barbara S. Lommer,[a]‡ Shoukath M. Ali,[b] Saroj N. Bajpai,[b] Wayne J. Brouillette,[b] Gillian M. Air[c] and Ming Luo[a,d]*

[a]Department of Microbiology, University of Alabama at Birmingham, Birmingham, AL 35294, USA, [b]Department of Chemistry, University of Alabama at Birmingham, Birmingham, AL 35294, USA, [c]Department of Biochemistry and Molecular Biology, University of Oklahoma, Oklahoma City, OK 73190, USA, and [d]Center for Biophysical Sciences and Engineering, University of Alabama at Birmingham, Birmingham, AL 35294, USA

‡ Current address: Max Planck Institute of Molecular Cell Biology and Genetics, 01307 Dresden, Germany.

Correspondence e-mail: mingluo@uab.edu

Received 11 February 2004
Accepted 16 March 2004

PDB Reference: BANA 207–B/Lee/40 NA complex, 1vcj, r1vcjsf.

Owing to the highly conserved nature of its active site, *Influenza B virus* neuraminidase (NA) has emerged as a major target for the design of novel anti-influenza drugs. A benzene-ring scaffold has been used in place of the pyranose ring of sialic acid to develop simpler NA inhibitors that contain a minimal number of chiral centers. A new compound belonging to this series, BANA 207, showed significant improvement in inhibitory activity against *Influenza B virus* NA compared with its parent compound. Here, the structural analysis of a complex of BANA 207 with influenza virus B/Lee/40 NA is reported. The results indicate that BANA 207 forms an unexpected interaction with the crucial active-site residue Glu275 that stabilizes the side chain of this residue in a conformation previously unobserved in NA–inhibitor complexes. This change in the side-chain orientation of Glu275 alters the topology of the triglycerol pocket, which accommodates an additional lipophilic substitution at the benzene ring and may provide an explanation for the increased activity of BANA 207 against *Influenza B virus* NA.

1. Introduction

Influenza virus neuraminidase NA (acetylneuraminyl hydrolase; EC 3.2.1.18) forms mushroom-shaped spikes on the surface of influenza virions and catalyzes the cleavage of α-ketosidic linkages between terminal sialic acid residues and adjacent sugars (Gottschalk, 1957; Laver & Valentine, 1969). The absence of active NA leads to extensive self-aggregation of the virus and termination of the infection since sialic acid acts as a receptor for viral hemaglutinin during virus attachment and is also present on the surface of newly budded virions (Eisen *et al.*, 1997; Palese *et al.*, 1974; Weis *et al.*, 1998).

Because of its well characterized active site, influenza virus NA has emerged as a major target for the design of novel anti-influenza drugs. Within its active-site cavity, which is structurally conserved in the NAs of both *Influenza A virus* and *Influenza B virus*, 11 highly conserved residues are located that interact with the sialic acid substrate (Bossart-Whitaker *et al.*, 1993; Burmeister *et al.*, 1992; Colman *et al.*, 1983; Ghate & Air, 1998; Goto *et al.*, 1997; Janakiraman *et al.*, 1994; Varghese *et al.*, 1992). Initial attempts to design inhibitors of NA concentrated on derivatives of sialic acid such as zanamivir (GG167), which became the first NA inhibitor to be approved for clinical use (Hayden *et al.*, 1997; von Itzstein *et al.*, 1999). However, the observation that the atoms of the sialic acid pyranose ring themselves did not seem to make crucial interactions with the active site opened the possibility of using different scaffolds from which functional groups could extend into the various binding sites of the active-site cavity. The most successful of these compounds, oseltamivir (GS4071), is based

Table 1
IC_{50} values of BANA 207 and its parent compound BANA 206.

Structures of BANA 207 and BANA 206 are shown in Fig. 1.

Inhibitor	NA	IC_{50}† (μ*M*)
BANA 206‡	A/Udorn/72 NA (N2)	0.49
	A/tern/Australia/G70c NA (N9)	4.4
	B/Lee/40 NA	271
BANA 207§	A/Udorn/72 NA (N2)	0.52
	A/tern/Australia/G70c NA (N9)	4.7
	B/Lee/40 NA	26

† Determined using the thiobarbiturate assay (Aymard-Henry *et al.*, 1973). ‡ Compound assayed as a 1:1 mixture of atropomers. § Compound assayed as an equimolar mixture of four diastereomers.

on a cyclohexene backbone (Kim *et al.*, 1997), but other scaffolds such as cyclopentane (Babu *et al.*, 2000) and pyrrolidine (Wang *et al.*, 2001) have also shown promise. Our group has concentrated on the development of inhibitors that employ a benzene-ring scaffold in an attempt to develop compounds that are more easily synthesized and that contain a minimal number of chiral centers.

Structural studies of complexes between several benzoic acid leads and a number of NAs revealed that these inhibitors were bound in the active site in a similar fashion to sialic acid (Jedrzejas *et al.*, 1995; Singh *et al.*, 1995). In these complexes, a carboxylate substitution extended from the benzene-ring scaffold into the positively charged binding site formed by Arg116, Arg292 and Arg374 (B/Lee/40 NA labeling). An *N*-acetyl substitution interacted with Arg150 and also formed hydrophobic contacts with parts of Trp177, Ile221 and Arg223, which are located opposite the arginine triad. In addition, using the benzene-ring scaffold, lipophilic groups could be fitted into the triglycerol-binding site through a rearrangement of the side chain of Glu275. However, attempts to bridge simultaneously from the benzene ring to both the negatively charged binding site formed by Glu117 and Asp149 and the triglycerol-binding site were unsuccessful, presumably owing to the fact that these pockets appear to be somewhat offset from the plane of the benzene ring (Atigadda *et al.*, 1999; Chand *et al.*, 1997; Finley *et al.*, 1999; Sudbeck *et al.*, 1997).

In an attempt to reach the negatively charged binding site indirectly from the benzene ring, a bis-(hydroxymethyl)-substituted pyrrolidinone ring was substituted for the *N*-acetyl group used in earlier benzene-ring compounds. This compound, termed BANA 206, exhibited potent activity against NAs of the N2 and N9 subtypes of *Influenza A virus* (Table 1; Fig. 1), but showed significantly less inhibitory activity against *Influenza B virus* NA, as observed previously for compounds that carried a similar lipophilic substitution at the benzene ring (Atigadda *et al.*, 1999). Recent efforts have been targeted at the optimization of BANA 206 in an attempt to create an inhibitor that shows broader activity for influenza virus NAs (Brouillette *et al.*, 2003). This report focuses on the interaction of one of the compounds obtained in this process, BANA 207, with *Influenza B virus* NA. Our findings indicate that the improved activity of BANA 207 against *Influenza B virus* NA is the result of an unexpected interaction with the side chain of Glu275, which was found to adopt a conformation that was previously unobserved in NA–inhibitor complexes.

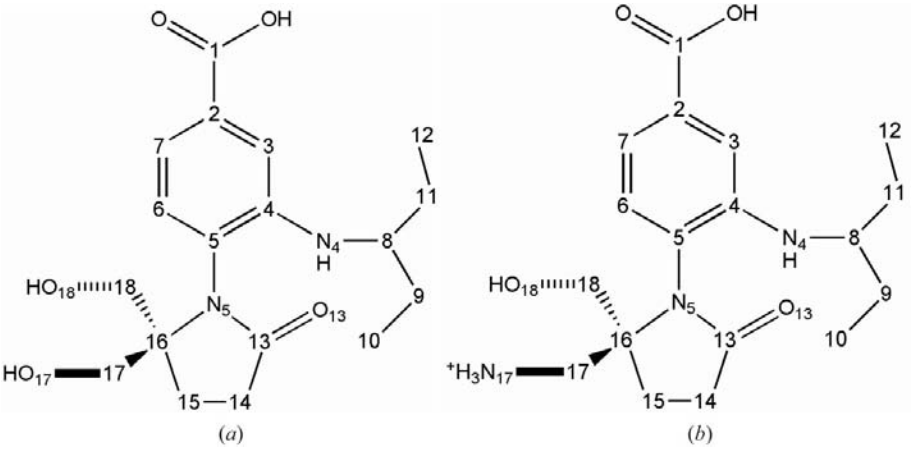

Figure 1
Chemical structures of (*a*) BANA 207 and (*b*) BANA 206.

2. Materials and methods

2.1. BANA 207

The synthesis, purification and evaluation of the *in vitro* inhibitory activity of BANA 207 {1-[4-carboxy-2-(3-pentylamino)phenyl]-5-aminomethyl-5-hydroxymethyl-pyrrolidin-2-one} has been described elsewhere (Brouillette *et al.*, 2003). BANA 207 is obtained as a 1:1 mixture of atropomers since free rotation about the bond between C5 and N5 is prevented by the benzene- and pyrrolidinone-ring substitutions. In addition, BANA 207 contains a chiral center at C16 such that four diastereomers of this inhibitors are produced. BANA 207 was introduced into crystals of B/Lee/40 NA as a mixture of these diastereomers.

2.2. Crystallization and data collection

B/Lee/40 virions were purified from allantoic fluid as described by Laver (1969). Subsequently, NA heads were released by trypsin digestion (Noll *et al.*, 1962; Wrigley *et al.*, 1977) and purified by size-exclusion chromatography using a Sephadex S-200 16/60 column (Pharmacia). Protein crystallization was carried out as described by Sudbeck *et al.* (1997) using an NA concentration of 3.0 mg ml^{-1} (Bradford method utilizing a bovine serum albumin standard curve) and a polyethylene glycol 3350 concentration of 18.5% in the well solution. BANA 207 was introduced into the NA crystals by soaking the crystals in soaking solution (1 m*M* BANA 207, 20% PEG 3350, 0.15 *M* NaCl, 2 *M* $NaNO_3$, 5 m*M* $CaCl_2$, 0.1% NaN_3 pH 6.8) for 16 h at 295 K. Data collection was carried

out at room temperature as described by Finley *et al.* (1999) using a HI-Star Multiwire detector (Bruker) and the data (400 frames) were processed using the *SADIE*/*SAINT* programs (Siemens Analytical X-ray systems, Inc). The diffraction data statistics are summarized in Table 2.

2.3. Structure determination and refinement

The crystals of the BANA 207–B/Lee/40 NA complex remained isomorphous with the crystals of a previously described complex of B/Lee/40 NA with sialic acid (Janakiraman *et al.*, 1994) and the coordinates of NA extracted from this earlier model were used to determine the structure of the present complex. The programs *X-PLOR* (Brünger *et al.*, 1998), *CNS* (Brünger *et al.*, 1998) and *QUANTA* (Molecular Simulations, Inc.) were used for all refinement and rebuilding operations and figures were generated using the program *RIBBONS* (Carson, 1997). 10% of the reflections were set aside as a test set for the calculation of $R_{\rm free}$. In addition, the geometry of the model was checked repeatedly using *PROCHECK* (Laskowski *et al.*, 1993). Reflections between 8 and 2.4 Å were used in all refinement steps and no $I/\sigma(I)$ cutoffs were employed. Topology and parameter files for the different diastereomers of BANA 207 were generated from *CHARMM* (Brooks *et al.*, 1983) minimized models of BANA 207 using *XPLO2D* (Kleywegt, 1995). Owing to the limited resolution of the data, all bond lengths and bond angles of BANA 207 were heavily restrained using weights of 4186 kJ mol^{-1} Å^{-2} and 2093 kJ mol^{-1} rad^{-2}, respectively. The benzene ring and the two sp^2-hybridized N atoms N4 and N5 were restrained to a flat geometry using weights of 3140 kJ mol^{-1} rad^{-2} for the appropriate improper angles. The same weight was used to restrain the chiral C atom C16 and a weight of 1256 kJ mol^{-1} rad^{-2} was used to limit the rotation about the bond between C5 and the pyrrolidinone ring, which is restricted because of steric hindrance. N17 was considered to be sp^3-hybridized based on nuclear magnetic resonance studies of BANA 207 (Brouillette *et al.*, 2003).

Refinement of the BANA 207–NA complex was initiated by rigid-body refinement of the protein component only, followed by several rounds of manual rebuilding and conventional positional refinement. Owing to the limited resolution of the data, harmonic restraints of 42 kJ mol^{-1} Å^{-2} were added to all C^{α} atoms and harmonic restraints of 21 kJ mol^{-1} Å^{-2} were added to all other atoms to avoid inappropriate movements of these atoms from their high-resolution positions. Subsequently, $F_{\rm o} - F_{\rm c}$ maps were calculated and models corresponding to the two diastereomers of BANA 207 that were consistent with the observed electron density were added. The positions of the inhibitor models were refined relative to the active site using rigid-body refinement. Next, $2F_{\rm o} - F_{\rm c}$ and $F_{\rm o} - F_{\rm c}$ omit maps were calculated that excluded the inhibitor models as well as all NA atoms within 8 Å of the inhibitor. Subsequently, several rounds of manual rebuilding and positional refinement were carried out as described above, with the exception that harmonic restraints of only 4.2 kJ mol^{-1} Å^{-2} were employed for all NA atoms located within 8 Å of the inhibitor. Water molecules were added to the complex if appropriate electron density could be observed in $F_{\rm o} - F_{\rm c}$ maps contoured at 2.0σ and in $2F_{\rm o} - F_{\rm c}$ maps contoured at 1.0σ and if visual inspection in *QUANTA* indicated that these molecules were located within hydrogen-bonding distance (2.5–3.5 Å) of at least one potential binding partner. Additional rounds of manual rebuilding, positional refinement and restrained individual *B*-factor refinement followed and the positions of individual active-site residues were confirmed using $F_{\rm o} - F_{\rm c}$ and $2F_{\rm o} - F_{\rm c}$ omit maps as well as SA-omit maps. The structure factors and model 2 of the BANA 207–B/Lee/40 NA complex have been deposited in the Protein Data Bank (PDB code 1vcj).

Table 2
Diffraction data and refinement statistics.

Values in parentheses refer to the highest resolution shell (2.40–2.49 Å). The refinement statistics are for BANA 207 model 2.

Space group	$P42_12$
Unit-cell parameters (Å)	$a = b = 124.36$, $c = 71.47$
No. unique reflections	18434
Resolution† (Å)	2.40
Completeness (%)	81.9 (63.2)
$I/\sigma(I)$	7.7 (2.6)
$I > 2\sigma(I)$ (%)	83.7 (59.4)
Redundancy	2.4 (1.6)
$R_{\rm sym}$ (%)	8.4 (20.7)
Crystallographic *R* factor (%)	21.4 (29.4)
$R_{\rm free}$ (%)	25.3 (32.3)
Average *B* factors (Å^2)	
Protein main-chain atoms	12.7
Protein side-chain atoms	14.1
Inhibitor atoms	8.1
Solvent atoms (107 waters used)	22.7
R.m.s. deviations from ideality	
Bond distances (Å)	0.010
Bond angles (°)	1.689
Ramachandran plot (%)	
Most favorable regions	84.9
Additional allowed regions	14.5
Generously allowed regions	0.6
Disallowed regions	0.0
Estimated average coordinate error (Luzzati plot) (Å)	
Test set	0.355
Working set	0.289

† The effective resolution was defined as the highest resolution bin with $I/\sigma(I) > 2.0$ and a data completeness of >60%.

2.4. Analysis of inhibitor interactions

Potential interactions between BANA 207 and B/Lee/40 NA were assessed visually in *QUANTA*. In addition, H atoms were added to the final coordinates of the complex and potential hydrogen-bond interactions, as well as hydrophobic contacts, were determined using *HBPLUS* (McDonald & Thornton, 1994). Potential hydrogen bonds were defined as interactions between donor and acceptor atoms that fulfilled the following geometric requirements: (i) a donor–acceptor distance (D-A) < 3.5 Å and a hydrogen–acceptor (H-A) distance of <2.5 Å and (ii) a donor–hydrogen–acceptor angle (D-H-A), a donor–acceptor–acceptor antecedent angle (D-A-

AA) and a hydrogen–acceptor–acceptor antecedent angle (H-A-AA) of >90° (Baker & Hubbard, 1984). Favorable hydrophobic contacts were defined as non-bonded contacts between two C atoms at a van der Waals distance of ∼4 Å (Copeland, 2000).

The model of the BANA 207–B/Lee/40 NA complex was compared with the model of native B/Lee/40 NA (Janakiraman *et al.*, 1994) and the model of the BANA 206–B/Lee/40 NA complex (Finley *et al.*, 1999) after superposition using the active-site backbone atoms only. Considering that the average Luzzati coordinate error for the BANA 207–B/Lee/40 complex was 0.29–0.36 Å, any root-mean-square deviations (r.m.s.d.s) of less than 0.5 Å were treated as insignificant.

3. Results

3.1. Inhibitor design and activity

Structural studies of BANA 206 in complex with NAs of both *Influenza A virus* and *Influenza B virus* revealed that its pyrrolidinone ring interacted with Arg150 as well as parts of Trp177, Ile221 and Arg223. However, its bis-(hydroxymethyl) substitutions formed only weak interactions with the active site and continued to leave the negatively charged binding site largely unoccupied (Atigadda *et al.*, 1999; Finley *et al.*, 1999).

Attempts to optimize BANA 206 therefore concentrated on the addition of various substitutions to the pyrrolidinone ring that were expected to undergo strong interactions with the negatively charged site. Interestingly, the most successful compound of this series, BANA 207, also carried the most conservative substitution: a single aminomethyl group in place of one of the hydroxymethyl groups of BANA 206 (Fig. 1, Table 1). This substitution did not affect its *in vitro* activity against NAs of the N2 and N9 subtypes of *Influenza A virus*. Intriguingly, however, BANA 207 exhibited a tenfold-improved activity against the NA of B/Lee/40 compared with its parent compound. This increase in activity was observed despite the fact that BANA 207 was assayed as a mixture of four stereoisomers (Brouillette *et al.*, 2003; Lommer, 2002).

3.2. Interactions of BANA 207 with B/Lee/40 NA

In an attempt to determine the interactions responsible for this increase in inhibitory activity against *Influenza B virus* NA, the structure of a complex between BANA 207 and B/Lee/40 NA was determined to a resolution of 2.4 Å. Initial $F_o - F_c$ maps showed clear electron density in the active site of NA and indicated that the pyrrolidinone ring was oriented in such a way as to bury its two substitutions inside the active site cavity (dihedral angle C6–C5–N5–C13 at the atropomeric center $\simeq -90°$). While this observation excluded two of the four possible stereoisomers of BANA 207, our data were not of sufficient resolution to distinguish between the hydroxymethyl and the aminomethyl groups themselves. Thus, two models of BANA 207 complexed with NA were generated to represent the two remaining stereoisomers of BANA 207 bound in the active site of NA. These models were refined to an R_{free} of 25.5 and 25.3%, respectively, and good stereochemistry was obtained for the protein chain in both cases, with only two residues (0.6%) present in the generously allowed regions of the Ramachandran plot. One of these residues, Trp408, is a second-shell active-site residue that indirectly interacts with BANA 207; the second, Asp384, is a surface residue that showed only weak density. All parts of the inhibitor models, the active-site residues of NA and the non-conserved residues Glu276 and Arg154 were well defined in $F_o - F_c$ and $2F_o - F_c$ electron-density maps that were generated by omitting the residue(s) in question from the phase calculation (Fig. 2). Overlays of the two stereoisomer models of BANA 207 showed no significant differences in overall conformation and location in the active site, with the corresponding groups of the inhibitor models exhibiting r.m.s.d.s that were smaller than the average coordinate error determined for both complexes according to the Luzzati method.

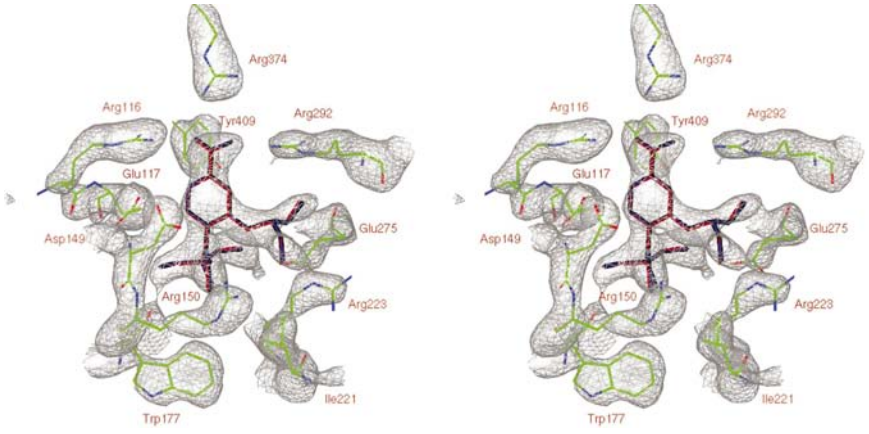

Figure 2
Stereoview of a $F_o - F_c$ omit map of BANA 207 and the conserved active-site residues of B/Lee/40 NA. BANA 207 and a sphere of 8 Å around it were omitted from the phase calculation and the map was contoured at 2σ. BANA 207 model 2 is shown in blue; the alternative model BANA 207 model 1 is shown in red. The NA side-chain atoms have been color-coded as follows: green, carbon; blue, nitrogen; red, oxygen.

Consistent with structural data obtained previously from other benzene-ring compounds, BANA 207 was bound in the active site through a number of strong charge-assisted hydrogen bonds between its carboxylate group and the arginine triad of the enzyme. Its pyrrolidinone ring interacted with Arg150 through a hydrogen bond and also showed some hydrophobic contacts with parts of Trp177, Ile221 and Arg223. The lipophilic side chain of BANA 207 extended into the triglycerol-binding site, where both of its branches formed van der Waals interactions of nearly ideal length with the side chains of Glu275, Ile221 and Arg223 (Table 3). The two pyrrolidinone-ring substitutions were found to occupy quite different chemical environments. One

substitution extended into a negatively charged pocket created by Glu275 and Glu276 and approached both groups close enough (2.8–3.3 Å) to indicate the formation of salt bridges or hydrogen bonds. The other substitution occupied a space near the carbonyl O atom of the backbone of Trp177 and the positively charged side chain of Arg154. The N atom of the aminomethyl substitution (N17) is sp^3-hybridized and positively charged at the pH at which crystallization and soaking of the inhibitor were carried out (pH 6.8). These observations indicate that it is this aminomethyl substitution that occupies the negatively charged area formed by Glu275 and Glu276, whereas the hydroxymethyl substitution forms hydrogen-bond interactions with Trp177 and the side chain of Arg154 (Fig. 3*b*; BANA 207 model 2). The opposite case, with the amine group occupying the space near Arg154, would be energetically less favorable owing to charge–charge repulsion between the amine group of BANA 207 and the side chain of Arg154. The hydroxyl group would also be in a less favorable environment in this case, because this group would approach two negatively charged groups at distances of 3.3 and 2.8 Å (Fig. 3*a*; BANA 207 model 1).

Table 3
Close contacts of the pyrrolidinone-ring substitutions and the aliphatic side chain of BANA 207 (model 2) with the active site of B/Lee/40 NA.

Inhibitor atom	NA atoms	Distance (Å)	Geometry favorable for hydrogen-bond formation
Pyrrolidinone-ring substitutions			
N17	Glu275 OE2	3.0	(N15)†‡
N17	Glu276 OE2§	3.0	(N15)†‡
O18	Trp177 O	2.6	(O16)†‡
O18	Arg154 NH§	3.1	—
C17	Glu226 CD, Glu226 CG	3.9	n.a.
C18	Glu226 CD, Trp177 C, Glu117 CD	4.0–4.2	n.a.
Aliphatic side chain			
C12	Asn294 CG§, Arg292 CD, Glu275 CG	4.0–4.2	n.a.
C11	Glu275 CG	4.2	n.a.
C9	Ala245 CB§	3.9	n.a.
C10	Arg223 CD, Ile221 CD1	3.9–4.0	n.a.

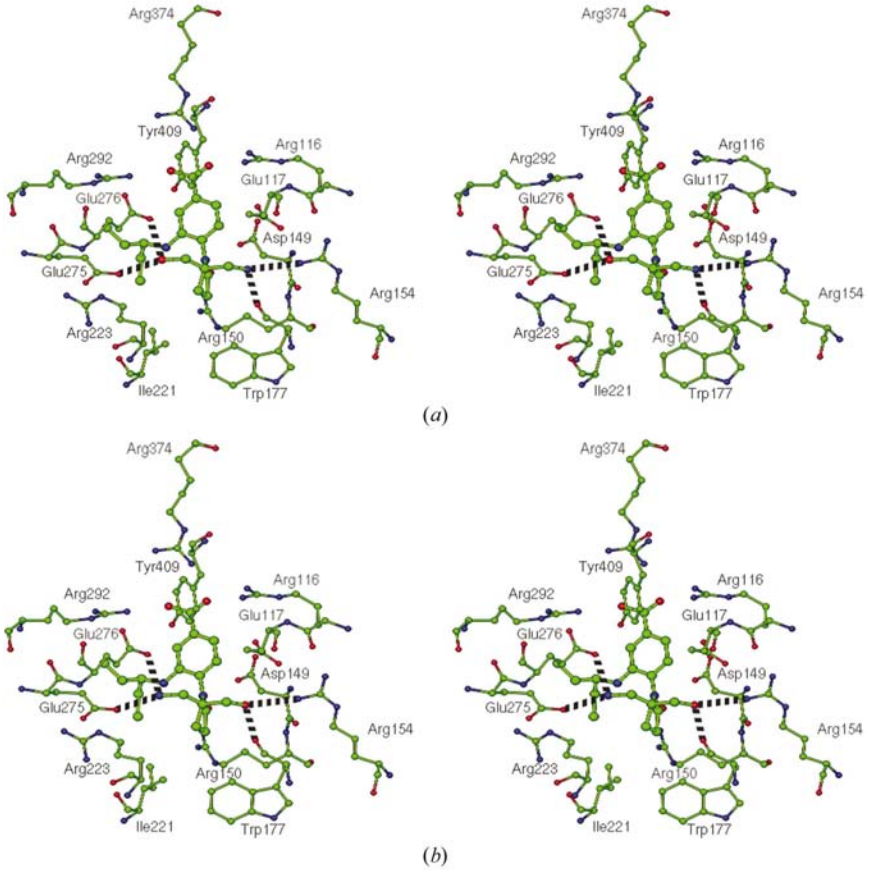

Figure 3
BANA 207 in the active site of NA. Stereoview. (*a*) BANA 207 model 1, (*b*) BANA 207 model 2. The elements are color-coded as follows: red, oxygen; blue, nitrogen; green, carbon. Potential interactions of the pyrrolidinone-ring substitutions are indicated by dotted lines.

3.3. Comparative analysis

Superposition of the active site of B/Lee/40 NA complexed with sialic acid (Janakiraman *et al.*, 1994) with the active site of the BANA 207–B/Lee/40 NA complex revealed only a few significant movements of active-site residues upon binding of BANA 207. The side chains of Glu226, Arg150 and Asp149 were pushed back somewhat (r.m.s.d. 0.5–0.6 Å at the terminal side-chain C atoms) to accommodate the inhibitor, but most active-site residues remained at their uncomplexed positions. The side chain of Glu275, however, showed a large conformational change that placed its carboxylate group farther into the active-site cavity and more than 3.7 Å away from its position in the absence of BANA 207 (r.m.s.d. 3.75 Å at atom CD; Fig. 4). In its new position, the carboxylate group of Glu275 forms a weak salt bridge with Arg223 NE (3.4 Å) in addition to its interaction with the aminomethyl substitution of BANA 207. Furthermore, in the BANA 207–B/Lee/40 NA complex the side chain of Glu275 replaces an active-site water molecule that is present near this location in the B/Lee/40 NA–sialic acid complex. A new water molecule is found near the original position of the Glu275 carboxylate group, which forms hydrogen bonds to the side chains of His273 (2.6 Å) and Arg223 (2.8 Å).

The conformation of the Glu275 side chain was also the most obvious difference when the BANA 207–B/Lee/40 NA complex was compared with the complex of its parent compound, BANA 206, with the same protein (Finley *et al.*, 1999). Although Glu275 was also rotated from its native

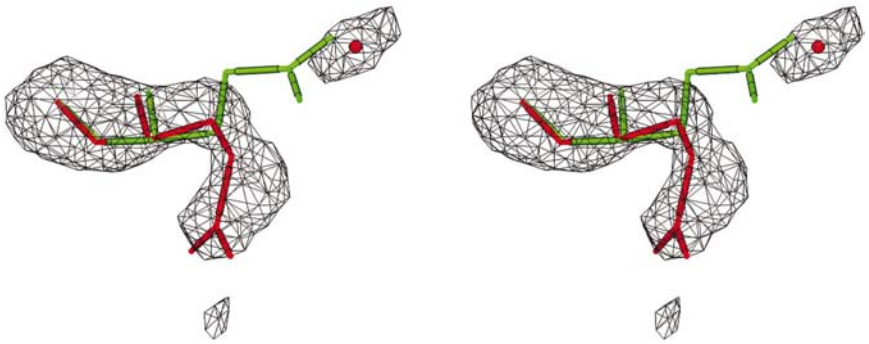

Figure 4
Stereoview of a $F_o - F_c$ omit map of Glu275 contoured at 2.5σ. Green, orientation of the side chain of Glu275 in the starting model (B/Lee/40 NA complexed with sialic acid). Red, fit of Glu275 to the density in the final model of the BANA 207–B/Lee/40 NA complex. A new water molecule is found near the former position of the Glu275 carboxyl group that forms hydrogen-bond interactions with His273 and Arg223. Both Glu275 and the water molecule were omitted for calculation of the electron density shown.

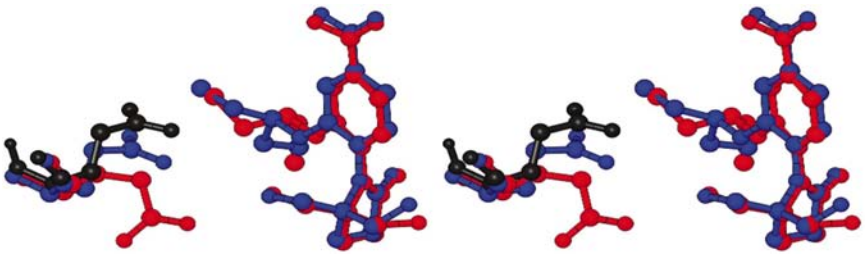

Figure 5
Superposition of BANA 207 and its parent compound BANA 206 (stereoview). BANA 207 is shown in red, while BANA 206 is depicted in blue. The orientation of Glu275 in the presence of the two inhibitors is shown using the same color-coding. The position of Glu275 in B/Lee/40 NA complexed with sialic acid is shown in black.

position in the presence of BANA 206, it was forced farther out of the active site and towards Arg223, with which it formed two strong charge-assisted hydrogen bonds. This rotation of the Glu275 side chain was in the opposite direction to that observed in the complex with BANA 207 (Fig. 5). Despite this difference in the conformation of Glu275, both inhibitors adopt a similar conformation overall and are bound in the same orientation in the active site. Further significant r.m.s.d.s were only observed in the conformation of their lipophilic side chains, especially at C11 (r.m.s.d. 0.96 Å) and C9 (r.m.s.d. 1.50 Å). As a consequence, the methyl group C10 of BANA 207 is directed into the active-site cavity, where it forms van der Waals interactions with both Arg223 and Ile221. The same group of BANA 206, in contrast, points away from the active-site cavity and does not make any interactions with other hydrophobic groups.

4. Discussion

A rotation of the side chain of Glu275 towards Arg223, like that observed in the complex between BANA206 and B/Lee/40 NA, has been reported in many complexes between NA and inhibitors carrying a lipophilic side chain (Atigadda *et al.*, 1999; Babu *et al.*, 2000; Finley *et al.*, 1999; Kati *et al.*, 2001; Kim *et al.*, 1997; Taylor *et al.*, 1998; Wang *et al.*, 2001). The extent of the disruption of the surrounding protein structure accompanying this conformational change of Glu275, however, is larger in *Influenza B virus* NA than in N9 NA. This difference in the topology of the triglycerol pocket is thought to be the cause of the difference in inhibitory activity against NAs of different influenza strains that is frequently observed for inhibitors carrying a lipophilic side chain targeted to this pocket (Atigadda *et al.*, 1999; Finley *et al.*, 1999; Taylor *et al.*, 1998). Like BANA 206, these compounds are typically significantly less active against *Influenza B virus* NA than against NAs from *Influenza A virus*. In the presence of BANA 207, however, the side chain of Glu275 was rotated in the opposite direction as observed previously, away from Arg223 and farther into the active-site cavity, where it appeared to be stabilized through an interaction with the aminomethyl group of BANA 207. This movement increased the size of the triglycerol pocket by effectively removing the Glu275 carboxylate group from the binding site and by fully exposing the hydrophobic atoms of its side chain. This change in the topography of the triglycerol pocket could at least partially be responsible for the improvement in inhibitory activity of *Influenza B virus* NA observed for BANA 207. Indeed, the largest differences between BANA 207 and BANA 206 were observed in the conformation of the lipophilic side chain, which is buried to a greater extent in BANA 207 than in BANA 206.

We thank J. Zhao for the preparation and purification of the B/Lee/40 virions, R. P. Mann for technical assistance and Drs C. D. Smith and J. B. Finley for technical assistance and helpful discussions. We are grateful to Dr A. Ball for a critical reading of this manuscript. This work was supported in part by NIH grant AI31888 (ML, WJB) and by a research grant from BioCryst Pharmaceuticals Inc.

References

Atigadda, V. R., Brouillette, W. J., Duarte, F., Ali, S. M., Babu, Y. S., Bantia, S., Chand, P., Chu, N., Montgomery, J. A., Walsh, D. A., Sudbeck, E. A., Finley, J., Luo, M., Air, G. M. & Laver, G. W. (1999). *J. Med. Chem.* **42**, 2332–2343.
Aymard-Henry, M., Coleman, M. T., Dowdle, W. R., Laver, W. G., Schild, G. C. & Webster, R. G. (1973). *Bull. WHO*, **48**, 199–202.
Babu, Y. S., Chand, P., Bantia, S., Kotian, P., Dehghani, A., El-Kattan, Y., Lin, T.-H., Hutchison, T. L., Elliot, A. J., Parker, C. D., Ananth, S. L., Horn, L. L., Laver, G. W. & Montgomery, J. A. (2000). *J. Med. Chem.* **43**, 3482–3486.
Baker, E. N. & Hubbard, R. E. (1984). *Mol. Biol.* **44**, 97–179.

Bossart-Whitaker, P., Carson, M., Babu, Y. S., Smith, C. D., Laver, W. G. & Air, G. M. (1993). *J. Mol. Biol.* **232**, 1069–1083.
Brooks, B. R., Bruccoleri, R. E., Olafson, B. D., States, D. J., Swaminathan, S. & Karplus, M. (1983). *J. Comput. Chem.* **4**, 187–217.
Brouillette, W. J., Bajpai, S. N., Ali, S. M., Velu, S. E., Atigadda, V. R., Lommer, B. S., Finley, J. B., Luo, M. & Air, G. M. (2003). *Bioorg. Med. Chem.* **11**, 2739–2749.
Brünger, A. T., Adams, P. D., Clore, G. M., DeLano, W. L., Gros, P., Grosse-Kunstleve, R. W., Jiang, J.-S., Kuszewski, J., Nilges, M., Pannu, N. S., Read, R. J., Rice, L. M., Simonson, T. & Warren, G. L. (1998). *Acta Cryst.* D**54**, 905–921.
Burmeister, W. P., Ruigrok, R. W. & Cusack, S. (1992). *EMBO J.* **11**, 49–56.
Carson, M. (1997). *Methods Enzymol.* **278**, 493–505.
Chand, P., Babu, Y. S., Bantia, S., Chu, N., Cole, L. B., Kotian, P. L., Laver, W. G., Montgomery, J. A., Pathak, V. P., Petty, S. L., Shrout, D. P., Walsh, D. A. & Walsh, G. M. (1997). *J. Med. Chem.* **40**, 4030–4052.
Colman, P. M., Varghese, J. N. & Laver, W. G. (1983). *Nature (London)*, **303**, 41–44.
Copeland, R. A. (2000). *Enzymes: A Practical Introduction to Structure, Mechanism and Data Analysis*, 2nd ed. New York: Wiley–VCH.
Eisen, M. B., Sabesan, S., Skehel, J. J. & Wiley, D. C. (1997). *Virology*, **232**, 19–31.
Finley, J. B., Atigadda, V. R., Duarte, F., Zhao, J. J., Brouillette, W. J., Air, G. M. & Luo, M. (1999). *J. Mol. Biol.* **293**, 1107–1119.
Ghate, A. A. & Air, G. M. (1998). *Eur. J. Biochem.* **258**, 320–331.
Goto, H., Bethell, R. C. & Kawaoka, Y. (1997). *Virology*, **238**, 265–272.
Gottschalk, A. (1957). *Biochim. Biophys. Acta*, **23**, 645–646.
Hayden, F. G., Osterhaus, A. D., Treanor, J. J., Fleming, D. M., Aoki, F. Y., Nicholson, K. G., Bohnen, A. M., Hirst, H. M., Keene, O. & Wightman, K. (1997). *N. Engl. J. Med.* **337**, 874–880.
Itzstein, M. von, Wu, W. Y., Kok, G. B., Pegg, M. S., Dyason, J. C., Jin, B., Van Phan, T., Smythe, M. L., White, H. F., Oliver, S. W., Colman, P. M., Varghese, J. N., Ryan, D. M., Woods, J. M., Bethell, R. C., Hotham, V. J., Cameron, J. M. & Penn, C. R. (1999). *Nature (London)*, **363**, 418–423.
Janakiraman, M. N., White, C. L., Laver, W. G., Air, G. M. & Luo, M. (1994). *Biochemistry*, **33**, 8172–8179.
Jedrzejas, M. J., Singh, S., Brouillette, W. J., Laver, W. G., Air, G. M. & Luo, M. (1995). *Biochemistry*, **34**, 3144–3151.
Kati, W. M., Montgomery, D., Maring, C., Stoll, V. S., Giranda, V., Chen, X., Laver, W. G., Kohlbrenner, W. & Norbeck, D. W. (2001). *Antimicrob. Agents Chemother.* **9**, 2563–2570.
Kim, C. U., Lew, W., Williams, M. A., Liu, H., Zhang, L., Swaminathan, S., Bischofberger, N., Chen, M. S., Mendel, D. B., Tai, C. Y., Laver, W. G. & Stevens, R. C. (1997). *J. Am. Chem. Soc.* **119**, 681–690.
Kleywegt, G. J. (1995). *CCP4/ESF–EACBM Newsl. Protein Crystallogr.* **31**, 45–50.
Laskowski, R. A., MacArthur, M. W., Moss, D. S. & Thornton, J. M. (1993). *J. Appl. Cryst.* **26**, 283–291.
Laver, W. G. (1969). *Fundamental Techniques in Virology*. New York: Academic Press.
Laver, W. G. & Valentine, R. C. (1969). *Virology*, **38**, 105–119.
Lommer, B. S. (2002). PhD Thesis. The University of Alabama at Birmingham, AL, USA.
McDonald, I. K. & Thornton, J. M. (1994). *J. Mol. Biol.* **238**, 777–793.
Noll, H., Aouagi, T. & Orlando, J. (1962). *Virology*, **18**, 154–157.
Palese, P., Tobita, K., Ueda, M. & Compans, R. W. (1974). *Virology*, **61**, 397–410.
Singh, S., Jedrzejas, M. J., Air, G. M., Luo, M., Laver, W. G. & Brouillette, W. J. (1995). *J. Med. Chem.* **38**, 3217–3225.
Sudbeck, E. A., Jedrzejas, M. J., Singh, S., Brouillette, W. J., Air, G. M., Laver, W. G., Babu, Y. S., Bantia, S., Chand, P., Chu, N., Montgomery, J. A., Walsh, D. A. & Luo, M. (1997). *J. Mol. Biol.* **267**, 1–11.
Taylor, N. R., Cleasby, A., Singh, O., Skarzynski, T., Wonacott, A. J., Smith, P. W., Sollis, S. L., Howes, P. D., Cherry, P. C., Bethell, R., Colman, P. & Varghese, J. (1998). *J. Med. Chem.* **41**, 798–807.
Varghese, J. N., McKimm-Breschkin, J. L., Caldwell, J. B., Kortt, A. A. & Colman, P. M. (1992). *Proteins*, **14**, 327–332.
Wang, G. T., Chen, Y., Wang, S., Gentles, R., Sowin, T., Kati, W., Muchmore, S., Giranda, V., Stewart, K., Sham, H., Kempf, D. & Laver, W. G. (2001). *J. Med. Chem.* **44**, 1192–1201.
Weis, W., Brown, J. H., Cusack, S., Paulson, J. C., Skehel, J. J. & Wiley, D. C. (1998). *Nature (London)*, **333**, 426–231.
Wrigley, N. G., Laver, W. G. & Downie, J. C. (1977). *J. Mol. Biol.* **109**, 405–421.